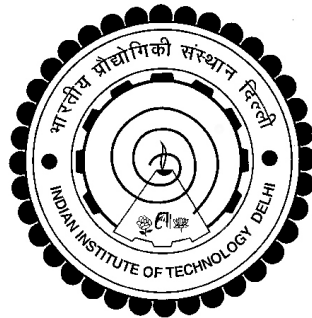


**STUDIES ON GRAPHENE BASED THERMOPLASTIC
POLYURETHANE NANOCOMPOSITES**

TARUNA BANSALA



**DEPARTMENT OF TEXTILE TECHNOLOGY
INDIAN INSTITUTE OF TECHNOLOGY DELHI
October 2017**

© Indian Institute of Technology Delhi (IITD), New Delhi, 2017

**STUDIES ON GRAPHENE BASED THERMOPLASTIC
POLYURETHANE NANOCOMPOSITES**

by

TARUNA BANSALA

Department of Textile Technology

Submitted

in fulfillment of the requirements of the degree of Doctor of Philosophy

to the



Indian Institute of Technology Delhi

October 2017

Dedicated to my family

CERTIFICATE

This is to certify that the thesis entitled, “**Studies on Graphene Based Thermoplastic Polyurethane Nanocomposites**” being submitted by **Ms. Taruna Bansala** to the Indian Institute of Technology Delhi, for the award of degree of **Doctor of Philosophy** is a record of bonafide research work carried out by him. **Ms. Taruna Bansala** has worked under my guidance and supervision and has fulfilled the requirements for the submission of this thesis, which to my knowledge has reached the requisite standard.

The results contained in this thesis are original and have not been submitted, in part or full, to any other University or Institute for the award of any other degree or diploma.

Dr. Mangala Joshi

Professor

Department of Textile Technology

Indian Institute of Technology Delhi

Hauz Khas, New Delhi-110016

Dr. Samrat Mukhopadhyay

Associate Professor

Department of Textile Technology

Indian Institute of Technology Delhi

Hauz Khas, New Delhi-110016

ACKNOWLEDGEMENTS

I wish to express my heartiest gratitude to my supervisors, Prof. Mangala Joshi and Dr. Samrat Mukhopadhyay for their invaluable guidance and constant encouragement. Their caring attitude and co-operation have been monumental throughout my research.

I am thankful to my SRC committee members Prof. A. K. Ghosh, Prof. Ashwini Aggarwal and Dr. Bhanu Nandan for their valuable suggestions and peer reviews.

I am also thankful to all the faculty members of Department of Textile Technology for their constant encouragement and help throughout my research work.

I express my thanks to Centre of Polymer Science and Technology, IIT Delhi, India, for providing facilities to carry out experiments in their lab.

It is a pleasure for me to express my gratitude towards all my lab mates. Their warm affection, support during tough times, nice scientific interactions, involvement and conscious as well as unconscious help have rendered my research life a bountiful time. I would like to thank all my seniors Dr. Kasturi Saha, Dr. Amitava Bhattacharyya, Dr. Pawan Verma, Dr. Sandeep Tripathi, Dr. Meenakshi Verma my colleagues, Bapan Adak, Vikas Singh, Anasuya Roy, Shilpi Sharma, Raghav Mehra, Sampat Singh, Gargi Jaiswal from IIT Delhi for their constant encouragement.

My special thanks to all the lab staff members for their immediate help whenever needed.

My family members especially my mother Smt. Anita Bansala deserve special attention for their support and persistent confidence in me, but I don't have words to express my gratitude for them.

I express my heartiest thanks to my husband, Pankaj Satwal for his constant support, encouragement and patience which enable me to pursue my career.

Finally, I would like to thank everyone who helped me in the successful compilation of thesis, as well as expressing my apology that I could not mention personally one by one.

I would like to acknowledge the financial assistance received from “MHRD” which has helped me to pursue my PhD without any stress.

Last but not the least I am thankful to the Almighty God in helping me to accomplish this task.

Taruna Bansala

ABSTRACT

In this study, three different type of graphene sheets such as thermally reduced graphene (TRG); chemically reduced graphene (CRG) and Polyvinyl-pyrrolidone stabilized silver nanoparticles based graphene nanohybrid (Ag-PVP-CRG) have been synthesized through thermal exfoliation and chemical processes respectively. These different graphene sheets have been characterized and studied for electromagnetic interference (EMI) shielding in microwave region. Further, TRG, CRG and Ag-PVP-CRG sheets have been dispersed in thermoplastic polyurethane (TPU) polymeric matrix to create multifunctional nanocomposite films through solution casting route. The study presents for the first time a comparative evaluation of three different types of graphene sheets for multifunctional properties in both neat and nanocomposite form. The synthesis and characterization of Ag-PVP-CRG nanohybrids and its investigation for such an application are also novel.

Graphite powder was functionalized into graphene oxide (GO). Firstly, GO was chemically reduced using hydrazine hydrate reduction to form CRG sheets. The oxygenic functional groups of GO were reduced to restore the graphitic structure in CRG sheets. Secondly, the GO was thermally reduced, exfoliated and annealed at 800 °C (rate 30 °C/min.) under N₂ atmosphere to obtain TRG sheets. Thirdly, Poly-vinyl-pyrrolidone (PVP) stabilized silver nanoparticles (AgNP) decorated graphene nanohybrid was synthesized from GO through chemical route synthesis in DMF/H₂O medium. The presence of silver nanoparticles onto the CRG sheets studied through high resolution transmission electron microscopy (HR-TEM).

Morphological studies on CRG, TRG and Ag-PVP-CRG nanohybrid revealed stacked multiple-layered CRG sheets, highly wrinkled exfoliated TRG nanosheets and PVP-stabilized AgNPs (15-30 nm) decorated graphene sheets respectively. The three different graphene sheets

were studied and compared for EMI shielding, dielectric and electrical conductivity properties. EMI shielding effectiveness (SE) attenuation was found to be highest for CRG (-80 dB), due to the stacked sheet structures, which provide 3D features resulting in highest conductivity (124.9 Scm^{-1}) and high dielectric losses. Decrease in stacking observed between nanosheets in TRG, due to high exfoliation process, lower electrical conductivity (62.74 Scm^{-1}) along with moderate dielectric losses and, therefore, lower EMI SE values (-45 dB). The lowest conductivity value (0.25 Scm^{-1}) obtained for Ag-PVP-CRG nanohybrid is attributed to the addition of PVP polymer. Additionally, observation of increased effective dielectric properties for Ag-PVP-CRG nanohybrid contributes to its EMI SE value of -58 dB. Further, these three different types of graphene sheets such as CRG, TRG and Ag-PVP-CRG have been used to prepare TPU based multi-functional nanocomposite films for various performance evaluations.

Initially, the conventional CRG sheets based TPU (TPU/CRG) nanocomposite films have been characterized and their performance properties such as electrical conductivity, EMI shielding, dielectric properties, gas barrier etc. have been evaluated. SEM revealed the presence of dispersed and agglomerated CRG sheets in TPU/CRG nanocomposite films, at higher conc. These films showed improved EMI shielding, dielectric properties and electrical conductivity. It was observed that the EMI shielding strongly correlates with the thickness of the films and the filler concentration loaded in the film. Thus, a large range of filler conc. varying from 1 to 20 wt.% and 2 mm thick films were studied. The poor dispersion and agglomeration of CRG sheets inside the TPU matrix was reflected in the increment in AC electrical conductivity and dielectric properties at very high conc. of CRG sheets 20 wt.%. However, DC electrical theoretical percolation threshold of 3.03 wt.% was observed for TPU/CRG nanocomposites films. The dielectric constant and tangent losses both increases with CRG conc. in TPU/CRG

nanocomposites. The prepared 20 wt.% TPU/CRG nanocomposite showed highest EMI SE of -18 to -20 dB in Ku (12.4 – 18 GHz) band radar frequencies. The gas barrier property of TPU/CRG nanocomposites films showed 60% reduction in N₂ gas permeability as compared to neat TPU film.

Thermally reduced and annealed graphene based thermoplastic polyurethane (TPU/TRG) nanocomposites films showed smooth morphology and fine dispersion of exfoliated TRG sheets inside the TPU matrix, when characterized through SEM, C-AFM, Raman spectroscopy and XRD. C-AFM studies confirmed the presence of electrically conducting TRG graphene sheets on the surface, as the current flow through TRG sheets protruding out of the TPU matrix. A low DC electrical percolation threshold of 1.49 wt.% was obtained, presumably attributed to the formation of 3D continuous electrical network of TRG nanosheets throughout the polymeric matrix. AC conductivity was found to be dominated by both charge mobility and frequency induced dielectric dispersion in TPU/TRG nanocomposite for TRG loading > 4 wt.%. The dielectric constant and tangent losses both increase with TRG conc. in TPU/TRG nanocomposites. The fabricated 10 wt.% TPU/TRG nanocomposite showed an excellent EMI SE of -26 to -32 dB in Ku (12.4–18 GHz) band. Because of large surface area of TRG sheets, the gas barrier property of TPU/TRG nanocomposite showed 99% reduction in N₂ gas permeability as compared to bare TPU matrix.

The TPU nanocomposite films based on Ag-PVP-CRG were characterized and an extensive assessment of EMI shielding, dielectric properties, electrical conductivity, and gas barrier property was carried out. The addition of AgNPs along with CRG sheets marginally improvised the dielectric properties and electrical conductivity of TPU matrix. The low increment in electrical conductivity and dielectric properties is due to poor dispersion and

agglomeration of CRG sheets inside the polymer matrix supported by SEM analysis and PVP coating on AgNPs which further reduced its conductivity. The highest DC conductivity value was obtained at 20 wt.% of TPU/Ag-PVP-CRG nanocomposites. The dielectric constant marginally increases but tangent losses were comparatively higher with Ag-PVP-CRG conc. in TPU/Ag-PVP-CRG nanocomposites. The fabricated 20 wt.% TPU/ Ag-PVP-CRG nanocomposite showed lowest SE of ~ -10 dB, in Ku (12.4 – 18 GHz) band radar frequencies. The gas barrier property of TPU/Ag-PVP-CRG was found to be moderate against nitrogen gas. This study shows that the type of graphene has a significant effect on its exfoliation and dispersion in TPU matrix which in turn is reflected in property differences between TPU/CRG, TPU/TRG and TPU/Ag-PVP-CRG nanocomposites in terms of electrical conductivity, dielectric behavior and finally EMI shielding potential.

सार

इस अध्ययन में, तीन अलग-अलग प्रकार की ग्राफीन शीट जैसे कि थर्मल ग्राफीन (TRG); कृत्रिम रूप से अपचयन ग्राफीन (CRG) और पॉलीविनाइल-पियरोलीडोन स्थिर चांदी के नैनोकणों पर आधारित ग्राफीन नैनोहेड्रिड (Ag-PVP-CRG) को क्रमशः थर्मल एक्सफोलेशन और रासायनिक प्रक्रियाओं के माध्यम से संश्लेषित किया गया है। माइक्रोवेव क्षेत्र में विद्युत चुम्बकीय हस्तक्षेप (EMI) के संरक्षण के लिए ये अलग-अलग ग्राफीन शीटों की विशेषता है और उनका अध्ययन किया गया है। इसके अलावा, TRG, CRG और Ag-PVP-CRG शीट को थर्मोप्लास्टिक पॉलीयूरेथेन (TPU) पॉलिमरिक मैट्रिक्स में डिसपर्स किया गया है जिससे सल्यूशन कास्टिंग मार्ग के माध्यम से बहुक्रियात्मक नॉनकोम्पॉजिट फिल्म तैयार की जा सके। अध्ययन ने साफ और नॉनकोम्पॉजिट रूप दोनों में बहुआयामी गुणों के लिए तीन अलग-अलग प्रकार की ग्राफीन शीटों की तुलनात्मक मूल्यांकन के लिए पहली बार प्रस्तुत किया है। एजी-पीवीपी-CRG नैनोहेड्रिड के संश्लेषण और लक्षण वर्णन और इस तरह के एक आवेदन के लिए इसकी जांच भी उपन्यास है।

ग्रेफाइट पाउडर को ग्राफीन ऑक्साइड (GO) में कार्यान्वित किया गया था। सबसे पहले, GO को CRG शीट बनाने के लिए हाइड्रोजीन हाइड्रेट में कमी का उपयोग करके रासायनिक रूप से कम किया गया। CRG शीट्स में ग्राफिक संरचना को पुनर्स्थापित करने के लिए ऑक्सिजनिक कार्यात्मक समूहों को कम किया गया। दूसरे, TRG को प्राप्त करने के लिए एनओ वायुमंडल के तहत 800 डिग्री सेल्सियस (दर 30 डिग्री सेल्सियस / मिन।) में GO को कम किया गया, एक्सफोलेशन और अनीलिंग किया गया। तीसरा, पॉलीविनील-पीरॉरिओडोन (PVP) स्थिर रजत नैनोकणों (AgNps) को सजाया गया, जीपीएन नैनोहेड्रिड GO से DMF /H₂O ओ माध्यम में रासायनिक मार्ग संश्लेषण के माध्यम से संश्लेषित किया गया था। CRG शीट पर चांदी नैनोकणों की उपस्थिति उच्च संकल्प संचरण इलेक्ट्रॉन माइक्रोस्कोपी (HRTEM) के माध्यम से अध्ययन किया।

CRG, TRG और Ag-PVP-CRG नैनोहेड्रिड पर आकृति विज्ञान संबंधी अध्ययनों ने क्रमशः कई स्तरित CRG शीट, अत्यधिक एक्सफोइएटेड TRG नैनोसाईट्स और PVP-स्थिर AgNP (15-30 nm) सजाए गए ग्राफीन शीट क्रमशः प्रकट किये। तीन अलग-अलग ग्राफीन शीट का अध्ययन किया गया और EMI के परिरक्षण, ढांकता हुआ और विद्युत चालकता गुणों के साथ तुलना की गई। EMI परिरक्षण प्रभावशीलता (SE) क्षीणन CRG (-80 dB) के लिए उच्चतम पाया गया, स्टैकड शीट संरचनाओं के कारण,

जो 3D विशेषताओं को प्रदान करता है जिसके परिणामस्वरूप उच्चतम चालकता (124.9 cm^{-1}) और उच्च ढांकता हुआ हानि होती है। उच्च छूटने की प्रक्रिया, निचले विद्युत चालकता (62.74 cm^{-1}) के कारण मध्यम ढांकता हुआ घाटे के साथ TRG में नैनोसेथेट्स के बीच मनाया जाने वाला स्टैकिंग, और इसलिए, कम EMI SE मान (-45 dB) में कमी। Ag-PVP-CRG नैनोहेइब्रिड के लिए प्राप्त न्यूनतम चालकता मूल्य (0.25 cm^{-1}) PVP बहुलक के अतिरिक्त के लिए जिम्मेदार है। इसके अतिरिक्त, Ag-PVP-CRG नैनोहेबिरिड के लिए प्रभावी प्रभावी ढांकता हुआ गुणों का अवलोकन -58 dB के अपने EMI SE मान में योगदान देता है। इसके अलावा, CRG, TRG और Ag-PVP-CRG जैसे ग्रेफाइन शीट्स के इन तीन अलग-अलग प्रकारों का उपयोग विभिन्न प्रदर्शन मूल्यांकन के लिए TPU आधारित बहुआयामी नैनोकोमोसाइट फिल्म तैयार करने के लिए किया गया है।

प्रारंभ में, पारंपरिक CRG शीट्स आधारित TPU (TPU / CRG) नैनोकोमोसाइट फिल्मों की विशेषता है और उनका प्रदर्शन गुण जैसे कि विद्युत चालकता, EMI परिरक्षण, ढांकता हुआ गुण, गैस बाधा आदि का मूल्यांकन किया गया है। EMI ने उच्च संगीता में TPU / CRG नैनोकोमोसाइट फिल्मों में छितरी हुई और एकत्रीकृत CRG शीट की उपस्थिति का खुलासा किया। इन फिल्मों में EMI परिरक्षण, ढांकता हुआ गुण और विद्युत चालकता दिखाया गया है। यह देखा गया कि EMI का परिरक्षण फिल्म की मोटाई के साथ दृढ़ता से संबंध रखता है और फिल्म में भरी हुई एकाग्रता के साथ जुड़ा हुआ है। इस प्रकार, भराव conc की एक बड़ी रेंज 1 से 20 wt.% और 2 mm मोटी फिल्मों का अध्ययन किया गया। TPU मैट्रिक्स के भीतर CRG शीट्स के खराब फैलाव और ढेर एसी बिजली चालकता और ढांकता हुआ गुणों में बढ़ोतरी में बहुत उच्च संलयन में दर्शाया गया था। CRG शीट्स का 20%wt. हालांकि, TPU/ CRG नैनोकोमोसाइट्स फिल्मों के लिए DC विद्युत सैद्धांतिक सैद्धांतिक झुकने की सीमा 3.03% थी। ढांकता हुआ निरंतर और स्पर्शरेखा नुकसान दोनों CRG कॉन्सर्ट के साथ बढ़ जाता है TPU / CRG नैनोकोमोसाइट्स में तैयार 20 wt.% TPU / CRG नैनोकोमोसाइट ने क्यू में -18 से -20 dB के उच्चतम ईएमआई एसई ($12.4 - 18 \text{ GHz}$) बैंड रडार आवृत्तियों को दिखाया। TPU / CRG नैनोकॉम्पोजिट फिल्मों की गैस बाधा की संपत्ति ने साफ TPU फिल्म की तुलना में N_2 गैस पारगम्यता में 60% कमी देखी।

थर्मलली कम और एनेल्ड ग्राफीन आधारित थर्मोप्लास्टिक पॉलीयूरेथेन (TPU / TRG) नैनोकोमोस्पेट्स फिल्मों में TPU मैट्रिक्स के अंदर छानने वाली TRG शीट्स की चिकनी आकृति विज्ञान और ठीक फैलाव दिखाया गया था, जब SEM, C-AFM, रमन स्पेक्ट्रोस्कोपी और XRD के जरिए चित्रित किया गया था। सी-एफएम अध्ययनों ने सतह पर TRG ग्रेफेन शीटों के विद्युत रूप से संचालित होने की पुष्टि की,

क्योंकि TPU मैट्रिक्स से निकलने वाली TRG शीट्स के माध्यम से मौजूदा प्रवाह के रूप में 1.49 wt.% की एक कम डीसी इलेक्ट्रिकल टपकन थ्रेसहोल्ड प्राप्त की गई, संभवतः पूरे पॉलिमर मैट्रिक्स में TRG नैनो शीट्स के 3D सतत इलेक्ट्रिकल नेटवर्क के गठन के लिए जिम्मेदार ठहराया गया। एसी चालकता दोनों चार्ज गतिशीलता और आवृत्ति के द्वारा प्रभुत्व पाया गया था

Table of Contents

Certificate	i
Acknowledgements	iii
Abstract	v
Table of content	x
List of figures	xviii
List of tables	xxv
List of symbols	xxvii
List of Abbreviations	xix
CHAPTER 1.....	1
INTRODUCTION AND OBJECTIVE OF WORK	
1.1 General	1
1.2 Motivation	5
1.3 Objective of the work	7
1.4 Outline of the thesis	8
CHAPTER 2.....	12
LITERATURE REVIEW	
2.1 Basis of Electromagnetic Interference (EMI) Shielding	12
2.2 Total Shielding Effectiveness	14
2.3 EMI shielding in Ku band (12.4 – 18 GHz)	15
2.4 EMI shielding material requirements	16
2.5 Graphene sheets	18
2.6 Graphene: Synthesis and Properties	19
2.6.1 Bottom-Up Approach	19
2.6.2 Top-down approach	20
2.6.2.1 Mechanical Exfoliation in Solution	20
2.6.2.2 Modifications of Graphite and Graphene Precursors	21
(a) Graphite Oxide	21
(b) Graphene Oxide (GO)	22
2.6.3 Graphene via reduction of precursors	22
2.6.3.1 Chemically Reduced Graphene (CRG) platelets	22
2.6.3.2 Thermally reduced Graphene Oxide (TRG)	23

2.7	Electro-magnetic shielding studies on graphene/ modified graphene based structures	24
2.8	Graphene based polymer nanocomposites	26
2.9	Methods of Manufacturing Thermoplastic Polyurethane/Graphene Nanocomposites	28
2.9.1	Solution mixing	28
2.9.2	Melt intercalation	29
2.9.3	Insitu polymerization: synthesis of PU-graphene nanocomposites	29
2.10	Characteristic Properties of TPU/Graphene Nanocomposites	30
2.10.1	Electrical Conductivity of Graphene/TPU Nanocomposites	30
2.10.2	Dielectric properties of Graphene/TPU Nanocomposites	32
2.10.3	EMI shielding of Graphene/TPU Nanocomposites	34
2.10.4	Mechanical properties	37
2.10.5	Barrier Properties against Fluid and Gases	39
2.11	Graphene Coating with metallic layers for EMI shielding properties	41
2.12	Applications of Graphene based-TPU nanocomposites	42
2.13	Evaluation and testing of PU/graphene Nanocomposites	43
2.13.1	Evaluation of EMI shielding effectiveness	43
2.13.2	Experimental shielding effectiveness	44
2.13.3	Electrical conductivity measurements	45
2.13.4	AC conductivity and Dielectric measurements	47
2.13.5	Gas Barrier testing	48

CHAPTER 3.....49
SYNTHESIS AND CHARACTERIZATION OF DIFFERENT GRAPHENE NANO-SHEETS (CRG, TRG & AG-PVP-CRG) AND EVALUATION OF THEIR EMI SHIELDING PROPERTIES

3.1	Introduction	49
3.2	Synthesis of chemically reduced graphene (CRG), thermally reduced graphene (TRG) and PVP-stabilized AgNP-based graphene nanohybrid (Ag-PVP-CRG)	51
3.2.1	General	51
3.2.2	Materials and methods	51
3.2.2.1	Materials	51
3.2.2.2	Synthesis of Graphene Oxide (GO)	52
3.2.2.3	Reduction of GO with hydrazine hydrate: chemically reduced graphene	52
3.2.2.4	Thermal expansion and exfoliation of graphene oxide	53
3.2.2.5	Synthesis of PVP-stabilized AgNP-based graphene nanohybrid	53

3.2.2.6	Characterization	54
3.2.3	Results and discussion	56
3.2.3.1	Morphological characterization using SEM and HR-TEM	56
3.2.3.2	UV-visible absorption spectra	58
3.2.3.3	XRD analysis of graphene nanosheets	59
3.2.3.4	Raman spectroscopy of graphene nanosheets	61
3.2.3.5	XPS analysis of GO, TRG, CRG and Ag-PVP-CRG nanosheets	63
3.2.3.6	Thermogravimetric analysis of graphene nanosheets	67
3.2.3.7	DC electrical conductivity analysis of Graphene nanosheets	68
3.2.3.8	Fourier Transform Infrared Spectroscopy (FT-IR) analysis of GO, CRG, TRG and Ag-PVP-CRG	69
3.2.3.9	Brunauer Emmett Teller (BET) Surface Area Analysis	71
3.2.4	Summary	72
3.3	Shielding effectiveness and dielectric studies	72
3.3.1	General	72
3.3.2	EMI shielding from stacked graphene sheet structures	73
3.3.3	EMI shielding of Ag-PVP-CRG nanohybrid	76
3.3.4	Comparison of Microwave Spectroscopy: Shielding Effectiveness (Absorbance, Reflectance, and Total) of neat Graphene sheets in Ku band frequency region	81
3.3.5	Summary	84

CHAPTER 4.....85
TPU/GRAPHENE NANOCOMPOSITES – SYNTHESIS, CHARACTERIZATION AND EMI SHIELDING BEHAVIOR

4.1	Introduction	85
4.2	Preparation of different Graphene such as CRG, TRG and Ag-PVP-CRG based TPU nanocomposite films	89
4.2.1	Materials and Methods	89
4.2.2.1	Materials	89
4.2.2.2	Preparation of graphene-based thermoplastic polyurethane (TPU) nanocomposite films	89
4.2.2.3	Characterization	92
4.2.2	General	94
4.3	Thermoplastic polyurethane/ chemically reduced graphene (TPU/CRG) nanocomposite films	96
4.3.1	Optimization of Nanoparticle Dispersion	96

4.3.2	Structure and morphology of TPU/CRG nanocomposites	97
4.3.2.1	Fracture surface of nanocomposite films	97
4.3.2.2	Raman analysis of CRG and TPU/CRG nanocomposites	99
4.3.2.3	XRD Analysis of TPU/CRG nanocomposites	100
4.3.2.4	Thermogravimetric analysis (TGA) of TPU/CRG nanocomposites	102
4.3.2.5	Conducting Atomic Force Microscopy (C-AFM) of TPU/CRG nanocomposites	104
4.3.3	Performance Properties of Films	105
4.3.3.1	DC electrical properties of TPU/CRG nanocomposite	105
4.3.3.2	AC Conductivity of TPU/CRG nanocomposites	107
4.3.3.3	Dielectric spectroscopy of TPU/CRG nanocomposites	110
4.3.3.4	Microwave Spectroscopy: Shielding Effectiveness (Absorbance, Reflectance, and Total), Skin depth, Real and Imaginary parts of Permittivity	112
a	EMI shielding effectiveness	112
b	Skin depth	115
c	Dielectric properties of TPU/CRG nanocomposites in Ku- Band (12.4 – 18 GHz)	116
4.3.3.5	Mechanical Properties of TPU/CRG nanocomposites	119
4.3.3.6	Gas Barrier Property Analysis of TPU/CRG nanocomposites	121
4.3.4	Summary	122
4.4	Thermoplastic polyurethane/ thermally exfoliated and annealed graphene sheets (TPU/TRG) nanocomposite films	123
4.4.1	Optimization of Nanoparticle Dispersion	123
4.4.2	Structure and morphology of TPU/TRG nanocomposites	124
4.4.2.1	Fracture surface of nanocomposite films	124
4.4.2.2	Raman analysis of TRG and TPU/TRG nanocomposites	124
4.4.2.3	XRD Analysis of TPU/TRG nanocomposites	127
4.4.2.4	Thermogravimetric analysis (TGA) of TPU/TRG nanocomposites	128
4.4.2.5	Conducting Atomic Force Microscopy (C-AFM) of TPU/TRG nanocomposites	130
4.4.3	Performance Properties of Films	132
4.4.3.1	DC electrical properties of TPU/TRG nanocomposite	132
4.4.3.2	AC Conductivity of TPU/TRG nanocomposites	133
4.4.3.3	Dielectric spectroscopy of TPU/TRG nanocomposites	136
4.4.3.4	Microwave Spectroscopy: Shielding Effectiveness (Absorbance, Reflectance, and Total), Real and Imaginary	138

	parts of Permittivity	
	a EMI shielding effectiveness	138
	b Skin depth	141
	c Dielectric properties of TPU/TRG nanocomposites in Ku- Band (12.4 – 18 GHz)	142
	4.4.3.5 Mechanical Properties of TPU/TRG nanocomposites	145
	4.4.3.6 Gas Barrier Property Analysis of TPU/TRG nanocomposites	146
	4.4.4 Summary	147
4.5	Thermoplastic polyurethane/ PVP stabilized silver nanoparticles based graphene (TPU/Ag-PVP-CRG) nanocomposite films	149
	4.5.1 Optimization of Ag-PVP-CRG Nanohybrid Dispersion in TPU matrix	149
	4.5.2 Structure and morphology of TPU/Ag-PVP-CRG nanocomposites	150
	4.5.2.1 Fracture surface of nanocomposite films	150
	4.5.2.2 XRD Analysis of TPU/Ag-PVP-CRG nanocomposites	151
	4.5.2.3 Thermogravimetric analysis (TGA) of TPU/Ag-PVP-CRG nanocomposites	153
	4.5.3 Performance Properties of Films	154
	4.5.3.1 DC electrical properties of TPU/Ag-PVP-CRG nanocomposite	154
	4.5.3.2 AC Conductivity of TPU/Ag-PVP-CRG nanocomposites	156
	4.5.3.3 Dielectric spectroscopy of TPU/Ag-PVP-CRG nanocomposites	158
	4.5.3.4 Microwave Spectroscopy: Shielding Effectiveness (Absorbance, Reflectance, and Total), Skin depth, Real and Imaginary parts of Permittivity	160
	a EMI shielding effectiveness	160
	b Skin depth	163
	c Dielectric properties of TPU/Ag-PVP-CRG nanocomposites in Ku- Band (12.4 – 18 GHz)	164
	4.5.3.5 Mechanical Properties of TPU/Ag-PVP-CRG nanocomposites	167
	4.5.3.6 Gas Barrier Property Analysis of TPU/Ag-PVP-CRG nanocomposites	167
	4.5.4 Summary	169

CHAPTER 5.....171
TPU/GRAPHENE NANOCOMPOSITES BASED ON TRG, CRG AG-PVP-CRG: A
COMPARATIVE EVALUATION

5.1	Introduction	171
5.2	Comparative Analysis of Different Graphene sheets (CRG, TRG, Ag-PVP-CRG)	173
5.2.1	Comparison of DC electrical conductivity and Brunauer Emmett Teller (BET) Surface Area Analysis of Graphene nanosheets	173
5.2.2	Comparison of Microwave Spectroscopy: Shielding Effectiveness (Absorbance, Reflectance, and Total) of neat Graphene sheets in Ku band frequency region	174
5.3	Comparative Analysis of TPU/Graphene nanocomposites properties	176
5.3.1	Viscosity Analysis	176
5.3.2	Fracture surface of nanocomposite films (10wt.%)	177
5.3.3	DC Electrical conductivity of TPU/Graphene nanocomposite films	179
5.3.4	Dielectric spectroscopy of TPU/Graphene nanocomposites	182
5.3.5	Microwave Spectroscopy: Shielding Effectiveness (Absorbance, Reflectance, and Total), Absorption efficiency of TPU/Graphene nanocomposites	186
5.3.6	Mechanical Properties of TPU/Graphene nanocomposites	190
5.3.7	Gas Barrier Property Analysis of TPU/Graphene nanocomposites	192
5.4	Summary	194

CHAPTER 6.....196
SUMMARY, CONCLUSIONS AND FUTURE SCOPE

6.1	Introduction	196
6.2	Summary	197
a	Morphological and electrical characterization of Graphene sheets such as CRG, TRG and Ag-PVP-CRG	197
b	Electromagnetic interference shielding and dielectric properties of Graphene sheets	198
c	Morphological and electrical characterization of TPU/CRG nanocomposites	198
d	Electromagnetic interference shielding, dielectric, mechanical and dielectric properties of TPU/CRG nanocomposites	199
e	Morphological and electrical characterization of TPU/TRG nanocomposites	199
f	Electromagnetic interference shielding, dielectric, mechanical and dielectric properties of TPU/CRG nanocomposites	200
g	Morphological and electrical characterization of TPU/Ag-PVP-CRG	200

	nanocomposites	
h	Electromagnetic interference shielding, dielectric, mechanical and gas barrier properties of TPU/Ag-PVP-CRG nanocomposites	201
i	Comparative evaluation of TPU/Graphene nanocomposites	201
6.3	Future scope of work	204

List of Figures

Figure No.	Title	Page No.
Chapter 2		
2.1	Schematic explanation of EMI shielding	12
2.2	Schematic showing the wide range usage of Ku band	17
2.3	Molecular structure of graphene as sp^2 hybridized chicken wire pattern	19
2.4	Various graphite/graphite modified precursors	20
2.5	Schematic showing structural difference between layered graphite oxide and exfoliated graphene oxide (GO) platelets	23
2.6	Schematic showing EM wave propagation in graphite nanosheets and reduced graphene oxide (r-GO) nanosheets	25
2.7	DC surface resistance of melt-blended graphite/TPU composites (closed symbols, also in inset) and melt-blended, solution-mixed, and insitu polymerized TRG/TPU composites (open symbols)	32
2.8	Figure 2.8: (a) Ku Band region stainless steel mould, (b) Hydraulic press, (c) Mould inside the hydraulic press	46
2.9	Schematic of gas permeability tester: (1): Nitrogen gas supply, (2): valve, (3): sample to be clamped here, (4): ram, (5): air escape, (6): pressure gauge, (7): manometer	48
Chapter 3		
3.1	Schematic showing the preparation of TRG sheets	53
3.2	Schematic representation of the preparation of the Ag-PVP-CRG nanohybrid	54
3.3	SEM images at 5KX of (a) chemically reduced graphene (CRG), (b) thermally reduced graphene (TRG), inset shows exfoliated wrinkled morphology at high magnification and (c) Ag-PVP-CRG nanohybrid, inset shows AgNPs presence on graphene sheets	57

3.4	(a), (b) TEM images of CRG sheets at low and high magnification respectively, (c) SAED pattern of CRG sheets, (d) and (e) low and high magnification HR-TEM image of TRG sheets, (f) SAED electron diffraction pattern of TRG sheets	57
3.5	(a) TEM and (b) HRTEM image of Ag-PVP-CRG nanohybrid (inset shows lattice fringes and SAED pattern)	58
3.6	Comparative UV - Visible absorbance spectra of GO and Ag-PVP-CRG	59
3.7	(a) XRD of G-O, CRG and TRG ($\theta=10-40^\circ$), (b) XRD of Ag-PVP-CRG nanohybrid ($\theta= 10-70^\circ$)	60
3.8	(a) Raman spectra of graphite, GO, CRG and TRG, (b) Raman spectra for GO and Ag-PVP-CRG nanohybrid showing that the presence of silver nanoparticles on graphene enhances the intensity of D and G band	62
3.9	High-resolution XPS spectra of C1s and O1s for GO (a, b), CRG (c, d) and TRG (e, f), respectively	65
3.10	(a) XPS survey spectra of Ag-PVP-CRG and GO samples (b) magnified Ag 3d core level XPS spectrum of Ag-PVP-CRG, (c) and (d) deconvoluted high-resolution XPS C 1s core level spectra of GO and Ag-PVP-CRG respectively	66
3.11	Thermogravimetric (TGA) plots of graphite, GO, CRG, TRG and Ag-PVP-CRG nanohybrid in a N ₂ atmosphere	68
3.12	Comparative FTIR spectra of GO, CRG, TRG and Ag-PVP-CRG	71
3.13	Variation in EMI shielding effectiveness of GO, CRG and TRG (a) SE _T , (b) Absorption losses SE _A , (c) Reflection losses SE _R , (d) SE@ 15GHz and (e) Absorption efficiency with frequency for a 2.0 mm thick sample	74
3.14	Frequency dependence of (a) real and (b) imaginary parts of permittivity and (c) corresponding dielectric tangent loss of GO, CRG and TRG for a 2.0 mm thick sample	77
3.15	Variation in EMI shielding effectiveness (a) SE _T (b) SE _A (c) SE _R with frequency for Ag-PVP-CRG nanohybrid which are 0.5, 1.0, 1.5 and 2.0 mm thick, and (d) distribution of total, absorbance and reflectance loss in total SE with sample thickness	78

3.16	Frequency dependence of (a) real (ϵ') and imaginary (ϵ'') parts of permittivity and (b) corresponding dielectric tangent loss ($\tan \delta_e$) of AgNPs decorated CRG sheets for a 2.0 mm thick sample	79
3.17	Schematic representation of the proposed EMI shielding mechanism in Ag-PVP-CRG nanohybrid	81
3.18	EMI SE in terms of SE_T , SE_A and SE_R of TRG, Ag-PVP-CRG and CRG	83
Chapter 4		
4.1	Temperature and vacuum profile for the drying of nanocomposite films	91
4.2	Preparation of TPU/TRG nanocomposite films	91
4.3	Change in solution viscosity under different mixing conditions for CRG sheets	97
4.4	SEM micrographs of the fractured surfaces of (a) neat TPU, (b, and c) 1 wt.% TPU/CRG, (d, e) 4 wt.% TPU/CRG, and (f, g, h) 8 wt.% TPU/CRG at different magnifications	98
4.5	Raman spectra of CRG, TPU and TPU/CRG nanocomposites	99
4.6	XRD patterns of TPU/CRG nanocomposites	101
4.7	TGA analysis of the TPU/CRG nanocomposites	103
4.8	AFM images, C-AFM images and room-temperature I–V curves of TPU/CRG nanocomposite at (a, b, c) 2 wt.%, (d, e, f) 6 wt.% and (g, h, i) 10 wt.% using conductive-AFM under ambient conditions (Bias voltage applied ranges from -10 V to +10 V)	108
4.9	DC electrical conductivity TPU/CRG nanocomposites <i>vs.</i> loading of CRG nanosheets. Inset showing $\log(\sigma)$ <i>vs.</i> $\log(\rho - \rho_0)$ plot	107
4.10	AC conductivity measurements of TPU/CRG nanocomposites at 25 kHz	109
4.11	Variation of AC electrical conductivity as a function of frequency for TPU/CRG nanocomposites with increasing conc. of CRG nanosheets	109
4.12	Dielectric properties of the TPU/CRG nanocomposite films as a function of frequency: (a) dielectric constant, and (b) tangent loss	111
4.13	(a) EMI shielding effectiveness of TPU/TRG nanocomposites with frequency (Ku Band region), (b) variation in SE_T , SE_A and SE_R with TRG loading at 15 GHz (mid- frequency range), (c) variation in absorption efficiency	114

4.14	Variation of skin depth with frequency of the TPU/CRG nanocomposites	116
4.15	Frequency dependence of (a) real and (b) imaginary parts of permittivity and (c) dielectric tangent loss for TPU/CRG nanocomposites	118
4.16	Mechanical properties of TPU/CRG nanocomposites as a function of the graphene loading (wt.%) (a) Young's modulus and strain at break, and (b) tensile strength	120
4.17	Relative permeability of TPU/CRG nanocomposites with respect to pure TPU film	121
4.18	Change in solution viscosity under different mixing conditions for TRG sheets	123
4.19	SEM micrographs of the fractured surfaces of (a) neat TPU, (b, and c) 1 wt.% TPU/TRG, (d, e) 4 wt.% TPU/TRG, and (f, g, h) 8 wt.% TPU/TRG at different magnifications	125
4.20	Raman spectra of TRG, TPU and TPU/TRG nanocomposites	126
4.21	XRD patterns of TPU/TRG nanocomposites	128
4.22	TGA analysis of the TPU/TRG nanocomposites	129
4.23	AFM images, C-AFM images and room-temperature I–V curves of TPU/TRG nanocomposite at (a, b, c) 2 wt.%, (d, e, f) 6 wt.% and (g, h, i) 10 wt.% by conductive-AFM under ambient conditions. Bias voltage applied ranges from -10 V to +10 V	131
4.24	DC electrical conductivity TPU/TRG nanocomposites vs. loading of TRG nanosheets. Inset showing $\log(\sigma)$ vs. $\log(\rho - \rho_0)$ plot	133
4.25	AC conductivity measurements of TPU/TRG nanocomposites at 25 kHz	135
4.26	Variation of AC electrical conductivity as a function of frequency for TPU/TRG nanocomposites with increasing conc. of TRG nanosheets	135
4.27	Dielectric properties of the TPU/TRG nanocomposite films as a function of frequency: (a) dielectric constant, and (b) tangent loss	137
4.28	(a) EMI shielding effectiveness of TPU/TRG nanocomposites with frequency (Ku Band region), (b) variation in SE_T , SE_A and SE_R with TRG loading at 15	141

	GHz (mid- frequency range), (c) variation in absorption efficiency	
4.29	Variation of skin depth with frequency of the TPU/TRG nanocomposites	142
4.30	Frequency dependence of (d) real and (e) imaginary parts of permittivity and (f) dielectric tangent loss for TPU/CRG nanocomposites	144
4.31	Mechanical properties of TPU/TRG nanocomposites as a function of the graphene loading (wt.%) (a) Young's modulus and strain at break, and (b) tensile strength	146
4.32	Relative permeability of TPU/TRG nanocomposites with respect to pure TPU film	147
4.33	Change in solution viscosity under different mixing conditions for Ag-PVP-CRG nanosheets	150
4.34	SEM micrographs of the fractured surfaces of (a) neat TPU, (b) 1 wt.% TPU/Ag-PVP-CRG, (c, d) 4 wt.% TPU/Ag-PVP-CRG, and (e, f) 8 wt.% TPU/Ag-PVP-CRG at different magnifications	151
4.35	XRD patterns of TPU/Ag-PVP-CRG nanocomposites	152
4.36	TGA analysis of the TPU/Ag-PVP-CRG nanocomposites	153
4.37	DC electrical conductivity TPU/Ag-PVP-CRG nanocomposites vs. loading of Ag-PVP-CRG nanosheets	155
4.38	AC conductivity of TPU/Ag-PVP-CRG nanocomposites at 25 kHz.	157
4.39	Variation of AC electrical conductivity as a function of frequency for TPU/Ag-PVP-CRG nanocomposites with increasing conc. of Ag-PVP-CRG nanosheets	158
4.40	Dielectric properties of the TPU/Ag-PVP-CRG nanocomposite films as a function of frequency: (a) dielectric constant, and (b) tangent loss	160
4.41	(a) EMI shielding effectiveness of TPU/Ag-PVP-CRG nanocomposites with frequency (Ku Band region), (b) variation in SE_T , SE_A and SE_R with Ag-PVP-CRG loading at 15 GHz (mid- frequency range), (c) variation in absorption efficiency	162

4.42	Variation of skin depth with frequency of the TPU/Ag-PVP-CRG nanocomposites	163
4.43	Frequency dependence of (a) real and (b) imaginary parts of permittivity and (c) dielectric tangent loss for TPU/Ag-PVP-CRG nanocomposites	166
4.44	Mechanical properties of TPU/Ag-PVP-CRG nanocomposites as a function of the graphene loading (wt.%) (a) Young's modulus, (b) strain at break, and (c) tensile strength	168
4.45	Relative permeability of TPU/Ag-PVP-CRG nanocomposites with respect to pure TPU film	169
Chapter 5		
5.1	Solution viscosity of TPU/Graphene nanocomposites (dope tested after 5 hrs. stirring and 1 hr. of ultrasonication)	177
5.2	SEM micrographs of the fractured surfaces of (a) neat TPU, (b) 10 wt.% TPU/Ag-PVP-CRG, (c) 10 wt.% TPU/CRG, and (d) 10 wt.% TPU/TRG at 2KX magnification	178
5.3	DC electrical conductivity TPU/Graphene nanocomposites vs. loading of graphene nanosheets. Inset showing $\log(\sigma)$ vs. $\log(\rho - \rho_0)$ plot	181
5.4	Dielectric properties of the TPU/Graphene nanocomposite films as a function of frequency ($20 - 10^6$ Hz): (a) dielectric constant, (b) tangent loss, (c) dielectric constant @ 1kHz, and (d) tangent loss @1kHz	184
5.5	(a) EMI shielding effectiveness of TPU/graphene (TRG, CRG and Ag-PVP-CRG) nanocomposites with frequency (Ku Band region), (b) variation in SE_T , SE_A and SE_R with different graphene loading at 15 GHz (mid- frequency range), (c) variation in absorption efficiency	189
5.6	Mechanical properties of TPU/Graphene nanocomposites as a function of the graphene loading (wt.%) (a) Young's modulus, (b) tensile strength and (c) strain at break	191
5.7	Relative permeability of TPU/Graphene nanocomposites with respect to pure TPU film	193

List of Tables

Table no.	Title	Page no.
Chapter 2		
2.1	Shows the Microwave bands, their frequency domains and particular application areas	16
2.2	Summary of literature review on graphene nanosheets as EMI shielding material	26
2.3	Electrical conductivity of graphene based polyurethane nanocomposites	33
2.4	Comparison of dielectric properties of graphene based polyurethane composites	35
2.5	Summary of literature review on graphene based thermoplastic polyurethane nanocomposites as EMI shielding material in X and Ku Band	37
2.6	Gas and moisture permeability of graphene based TPU nanocomposites	40
Chapter 3		
3.1	Raman intensity peak of GO, CRG, TRG and Ag-PVP-CRG nanohybrid at G and D band	63
3.2	Summary of elemental composition of GO, CRG, TRG and Ag-PVP-CRG	64
3.3	Electrical conductivity values of graphene nanosheets	69
3.4	FTIR analysis of different types of graphene	70
3.5	BET surface area, pore volume and diameter of CRG and TRG	81
3.6	EMI shielding effectiveness summary of graphene sheets such as TRG, CRG and Ag-PVP-CRG @ 15 GHz	83
Chapter 4		
4.1	Materials used for film preparation	90
4.2	Compositions of different graphene based TPU	92

	nanocomposite samples	
4.3	Raman shift in CRG nanosheets, TPU/CRG nanocomposites (laser source 785 cm ⁻¹ wavenumber)	100
4.4	TGA analysis of TPU/CRG nanocomposites	103
4.5	Electromagnetic shielding properties of CRG based polymeric nanocomposite: a comparative evaluation	119
4.6	Raman shift in TRG nanosheets, TPU/TRG nanocomposites (laser source 785 cm ⁻¹ wavenumber)	127
4.7	TGA analysis of TPU/TRG nanocomposites	129
4.8	Comparison of dielectric properties of graphene based polyurethane composites	139
4.9	Comparative evaluation of electromagnetic shielding properties of graphene-based TPU nanocomposites	145
4.10	TGA Analysis of TPU/Ag-PVP-CRG nanocomposites	154
Chapter 5		
5.1	Summary of Electrical conductivity data and BET surface area for different types of graphene	174
5.2	Summary of EMI shielding effectiveness of different graphene nanosheets @ 15 GHz	176
5.3	Summary of Electrical conductivity data of different graphene (TRG, CRG and Ag-PVP-CRG) based TPU nanocomposites	182
5.4	Summary of dielectric properties of different graphene (TRG, CRG and Ag-PVP-CRG) based TPU nanocomposites	185
5.5	Summary of EMI shielding effectiveness of different graphene (TRG, CRG and Ag-PVP-CRG) based TPU nanocomposites @ 15GHz	190
5.6	Summary of Mechanical properties of different graphene (TRG, CRG and Ag-PVP-CRG) based TPU nanocomposites	192

List of symbols

θ	Bragg diffraction angle
$\tan \delta$	Tangent delta
μ	Permeability
σ	Conductivity
δ	Skin depth
ε	Dielectric permittivity

List of Abbreviations

TPU	Thermoplastic polyurethane
CNT	Carbon nanotubes
GO	Graphene oxide
CRG	Chemically reduced graphene sheets
TRG	Thermally reduced and annealed graphene sheets
Ag-PVP-CRG	PVP stabilized silver nanoparticles decorated graphene sheets
TGA	Thermogravimetric analysis
FT-IR	Fourier Transmission Infrared Spectroscopy
XRD	X-ray diffraction analysis
SEM	Scanning electron microscopy
TEM	Transmission electron microscopy
VNA	Vector network analyzer
EMI	Electromagnetic interference
SE_A	Absorption loss
SE_R	Reflection loss
SE_M	Multiple Reflections
SE_T	Total Shielding Effectiveness
AgNPs	Silver nanoparticles
PVP	Polyvinylpyrrolidone
C-AFM	Conducting Atomic Force Microscopy